

# Light-quark two-loop corrections to heavy-quark pair production in the gluon fusion channel

---

R. Bonciani<sup>1, a</sup>, A. Ferroglia,<sup>b</sup> T. Gehrmann,<sup>c</sup> A. von Manteuffel,<sup>dc</sup> C. Studerus<sup>e</sup>

<sup>a</sup>*INFN Sezione di Roma, Piazzale Aldo Moro 5, 00185 Roma, Italy*

<sup>b</sup>*Physics Department, New York City College of Technology, The City University of New York, 300 Jay Street Brooklyn, NY 11201 US*

<sup>c</sup>*Institute for Theoretical Physics, University of Zürich, Winterthurerstrasse 190, 8057 Zürich, Switzerland*

<sup>d</sup>*PRISMA Cluster of Excellence & Institute of Physics, Johannes Gutenberg University, 55099 Mainz, Germany*

<sup>e</sup>*Faculty of Physics, University of Bielefeld, Postfach 100131, 33501 Bielefeld, Germany*  
*E-mail: [roberto.bonciani@roma1.infn.it](mailto:roberto.bonciani@roma1.infn.it), [afferroglia@citytech.cuny.edu](mailto:afferroglia@citytech.cuny.edu),  
[thomas.gehrmann@uzh.ch](mailto:thomas.gehrmann@uzh.ch), [manteuffel@uni-mainz.de](mailto:manteuffel@uni-mainz.de),  
[cedricstuderus@gmail.com](mailto:cedricstuderus@gmail.com)*

**ABSTRACT:** We calculate the two-loop corrections to heavy-quark pair production in the gluon fusion channel which arise from diagrams involving a closed light-quark loop. The calculation is carried out by keeping the exact dependence on the heavy-quark mass. The analytic results are written in terms of logarithms, classical polylogarithms  $\text{Li}_n$  ( $n = 2, 3, 4$ ), and genuine multiple polylogarithms  $\text{Li}_{2,2}$ . The functional arguments are rational expressions of two independent external invariants and they are chosen in such a way that the functions are real in all the physical phase-space points. Through systematic changes in the functional basis, we obtain expansions of the results in both the production threshold and small mass limits.

---

<sup>1</sup>On leave of absence from Dipartimento di Fisica, Università di Roma “La Sapienza”.

---

## Contents

<b>1</b>	<b>Introduction</b>	<b>1</b>
<b>2</b>	<b>Notations and conventions</b>	<b>3</b>
<b>3</b>	<b>Calculational method</b>	<b>4</b>
3.1	Outline of the calculation	4
3.2	Renormalization	5
3.3	Multiple polylogarithms	6
<b>4</b>	<b>Analytic results</b>	<b>9</b>
<b>5</b>	<b>Expansions</b>	<b>11</b>
5.1	Threshold expansion	11
5.2	Small mass expansion	13
<b>6</b>	<b>Conclusions</b>	<b>16</b>
<b>A</b>	<b>Numerical samples</b>	<b>17</b>

---

## 1 Introduction

The production of top-antitop quark pairs is one of the processes which is measured with such a precision at the Large Hadron Collider (LHC) that, on the theoretical side, one needs to obtain predictions including perturbative corrections beyond the next-to-leading order (NLO) in QCD. Recently, the calculation of the full next-to-next-to leading order (NNLO) corrections to the total top-quark pair-production cross section was completed [1–4], based on a purely numerical framework for the calculation of the virtual corrections [5] and the real radiation subtractions [6, 7]. When these results are supplemented by the resummation of the threshold logarithmically-enhanced terms, due to the soft-gluon emission, at the next-to-next-to-leading logarithmic (NNLL) accuracy, the perturbative uncertainty at LHC center of mass energies is as low as 3% [4]. This is just a few percent smaller than the current experimental uncertainty.

NNLO QCD computations require the evaluation of tree-level diagrams with the emission of two additional partons in the final state (real corrections), of one-loop diagrams with an additional parton in the final state (real-virtual corrections) [8–12], and of two-loop diagrams without additional partons in the final state (virtual corrections). Each one of these three elements involves a large number of diagrams and, in top-quark pair production, it is further complicated by the need to account for the finite mass of the top-quark. The task of combining these elements and organizing the cancellation of the residual infrared

singularities among the various terms in a way which is efficient for numerical evaluation is itself very challenging [6, 7, 13–34].

In this paper we focus our attention on the analytic calculation of the two-loop corrections to heavy-quark hadroproduction. (In this context we will use the terms heavy quark and top quark interchangeably.) Even with purely numerical results available, there are strong motivations for an analytic calculation. Firstly, it facilitates a clearer understanding of the structure of the result. Furthermore, it offers particularly robust, fast and precise numerical evaluations for the theoretical predictions of the physical observables. Finally, it also provides an excellent cross check of the numerical calculations.

The two-loop QCD corrections to top-quark pair production were at first evaluated in the small mass limit [35, 36]. In those papers, terms proportional to positive powers of the heavy-quark mass  $m$  were neglected and  $m$  was only kept as a regulator of collinear singularities. The first diagrams to be calculated analytically by retaining the full dependence on the top-quark mass were the quark-annihilation channel diagrams involving a closed light- or heavy-quark loop [37]. Subsequently, the diagrams contributing to the leading color structure were evaluated in both the quark-annihilation [38] and gluon-fusion [39] channels. The calculations in [37–39] were carried out by identifying a set of Master Integrals (MIs) by means of the Laporta Algorithm [40–43], and by subsequently evaluating the MIs using the Differential Equations Method [44–51]. In order to carry out these calculations, a process independent, multi-purpose implementation of the Laporta Algorithm was written in C++, the package `Reduze`. This software employs functionalities from `GiNaC` [52] and `Fermat` [53] and it is now publicly available [54, 55]. The final analytic results were written in terms of Goncharov multiple polylogarithms or Generalized Harmonic Polylogarithms (GHPLs) [56–59], which contain the Harmonic Polylogarithms (HPLs) [60–67] as a subset. Expansions near the production threshold and in the small mass (high energy) limit were obtained for all of the results in [37–39].

In this paper we present the calculation of the gluon fusion channel two-loop diagrams involving a light (i.e. massless) quark loop. The analytic structure of the MIs involved in this calculation is more complicated than the one we encountered in the past. The most complicated MIs, needed for the two-loop box diagrams, were recently evaluated in [68–70] and require a significantly extended set of GHPLs. The analytic results for the light quark two-loop corrections allow for a clean extraction of the relevant real parts in the physical region, they are suitable for stable and fast numerical evaluations, and it is possible to expand them both in the production threshold limit  $s \rightarrow 4m^2$  and in the small mass limit  $m^2/s \rightarrow 0$ . In order to achieve all of these goals it was necessary to rewrite the results in terms of different functional bases, which is a non-trivial task. Symbol and coproduct based techniques for multiple polylogarithms were already proven to be powerful tools in various  $N = 4$  Super-Yang-Mills Theory and QCD applications [68, 69, 71–85]. Here, we extensively apply the coproduct-augmented symbol calculus presented in [74, 76] for our purpose. Ultimately, the corrections evaluated here are written in terms of logarithms, classical polylogarithms  $\text{Li}_n$  ( $n = 2, 3, 4$ ), and genuine multiple polylogarithms  $\text{Li}_{2,2}$ . All of these transcendental functions are real over the entire physical phase space.

The paper is organized as follows: in Section 2 we introduce our notation and conven-

tions. The calculational method is described in Section 3, which also includes a description of different functional bases used to represent our results at different stages of the calculation. The terms which are proportional to the number of light quarks  $N_l$  in the interference between the two-loop and tree-level amplitudes can be arranged in seven gauge-invariant color coefficients. The analytic expressions for these coefficients are discussed in Section 4. These results are too lengthy to be included in the text. For this reason we collect them in an ancillary file which we attach to the arXiv submission of this work. The expansion of the seven color coefficients near the production threshold and in the small mass limit is presented in Section 5. Section 6 contains our conclusions. In Appendix A, we supply numerical values for the considered color coefficients in a few phase space points.

## 2 Notations and conventions

In this paper we consider the two-loop corrections to the partonic scattering process

$$g(p_1) + g(p_2) \longrightarrow t(p_3) + \bar{t}(p_4), \quad (2.1)$$

where  $p_1^2 = p_2^2 = 0$  and  $p_3^2 = p_4^2 = -m^2$ . It is convenient to introduce the Mandelstam invariants, which are defined as follows:

$$s = -(p_1 + p_2)^2, \quad t = -(p_1 - p_3)^2, \quad \text{and} \quad u = -(p_1 - p_4)^2. \quad (2.2)$$

The invariants satisfy the momentum conservation relation  $s + t + u = 2m^2$ . The squared matrix element (summed over spin and colour) can be expanded in powers of the strong coupling constant  $\alpha_s$  according to

$$\sum |\mathcal{M}(s, t, m^2, \varepsilon)|^2 = 16\pi^2 \alpha_s^2 \left[ \mathcal{A}_0 + \frac{\alpha_s}{\pi} \mathcal{A}_1 + \left(\frac{\alpha_s}{\pi}\right)^2 \mathcal{A}_2 + \mathcal{O}(\alpha_s^3) \right]. \quad (2.3)$$

In Eq. (2.3), the argument  $\varepsilon = (4 - d)/2$  indicates the dimensional regulator. We suppressed the arguments  $s, t, m^2, \varepsilon$  in the functions  $\mathcal{A}_i$ . It must be remarked that after UV renormalization the terms  $\mathcal{A}_i$  ( $i \geq 1$ ) still include IR divergences, which are regulated by  $\varepsilon$ . These divergences cancel only after the virtual corrections are added to the real emission ones. The term  $\mathcal{A}_0$  in Eq. (2.3) arises from the interference of tree-level diagrams; its explicit expression is well known (see for example [39]). The term  $\mathcal{A}_1$  indicates the interference of one-loop and tree-level diagrams [86, 87]. The term  $\mathcal{A}_2$  can be further split in the sum of two contributions

$$\mathcal{A}_2 = \mathcal{A}_2^{(2 \times 0)} + \mathcal{A}_2^{(1 \times 1)}. \quad (2.4)$$

$\mathcal{A}_2^{(1 \times 1)}$  arises from the interference of one loop diagrams and was evaluated in [88–90]. The color structure of the interference of two-loop and tree-level diagrams,  $\mathcal{A}_2^{(2 \times 0)}$ , is the following

$$\mathcal{A}_2^{(2 \times 0)} = (N_c^2 - 1) \left\{ N_c^3 A + N_c B + \frac{1}{N_c} C + \frac{1}{N_c^3} D + N_c^2 N_l E_l + N_c^2 N_h E_h + N_l F_l + N_h F_h \right.$$

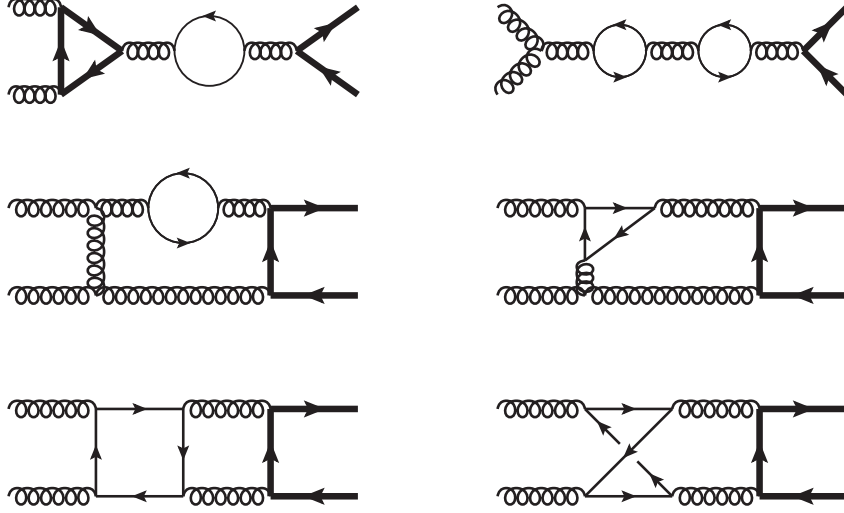


**Figure 1.** Some of the two-loop diagrams needed for the evaluation of the 7 color coefficients discussed in this paper. Thick fermion lines represent heavy quarks, thin fermion lines represent massless quarks. The diagrams in the first line contribute to color coefficients proportional to  $N_l N_h$  and  $N_l^2$ , respectively. The box diagrams in the last two lines contribute to the color coefficients proportional to  $N_l$ .

$$\begin{aligned}
 & + \frac{N_l}{N_c^2} G_l + \frac{N_h}{N_c^2} G_h + N_c N_l^2 H_l + N_c N_h^2 H_h + N_c N_l N_h H_{lh} + \frac{N_l^2}{N_c} I_l \\
 & + \left. \frac{N_h^2}{N_c} I_h + \frac{N_l N_h}{N_c} I_{lh} \right\}, \tag{2.5}
 \end{aligned}$$

where  $N_c$  indicates the number of colors,  $N_l$  the number of light (i.e. massless) flavor quarks and  $N_h$  the number of quarks of mass  $m$ . In the case of top-quark pair production one should set  $N_h = 1$ . The 16 gauge-invariant color coefficients  $A, B, \dots, I_{lh}$  are functions of  $s, t, m^2$  and  $\varepsilon$ . To date, only the leading color coefficient,  $A$ , was calculated analytically [39]. In the present work we evaluate the seven color coefficients proportional to  $N_l$ :  $E_l, F_l, G_l, H_l, H_{lh}, I_l$  and  $I_{lh}$ .

### 3 Calculational method

#### 3.1 Outline of the calculation

In this section we briefly summarize the way in which the calculation was organized and carried out. The two-loop Feynman diagrams which contribute to the  $gg \rightarrow t\bar{t}$  process were generated with **Qgraf** [91]. The total number of diagrams in this channel is 789. Diagrams involving a closed light-quark loop are counted only once and are multiplied by the number of light quarks. 126 diagrams are proportional to  $N_l$ , 6 are proportional to  $N_l N_h$ , and 3 are proportional to  $N_l^2$ . Some of the two-loop diagrams which we need to evaluate are shown in Fig. 1. Since in our calculation we set the sum over the gluon polarization vectors equal to the metric tensor, we need to add the contribution of the diagrams with incoming

Faddeev-Popov ghosts. This amounts to consider 31 additional diagrams proportional to  $N_l$ , 2 diagrams proportional to the product  $N_l N_h$ , and 1 diagram proportional to  $N_l^2$ . The **Qgraf** output becomes the input for **Reduze 2** [55]. The program starts by interfering the two-loop diagrams with the tree-level amplitude, and by subsequently calculating traces over color, spinor and Lorentz indices. By carrying out shifts on the integration momenta, **Reduze 2** assigns to each diagram a sector of an appropriate integral family (auxiliary topology). The list of the nine propagator integral families employed in this calculation is collected in the ancillary file `integralfamilies.yaml`, included in the arXiv submission of this paper. Finally, **Reduze 2** generates the system of Integration by Parts Identities (IBPs) and solves it, identifying the relevant set of MIs. The program handles multiple integral families at the same time and deals with crossings of external legs. It identifies shift relations between different sectors (sector relations) or integrals of the same sector (sector symmetries). Occasionally, sector symmetries provide information not included in the IBP identities. Some of the integrals needed in the calculation presented here were already available in the literature [92–102]. However, 11 integrals with two massive and two massless external legs had to be calculated specifically for this project. Their evaluation has many interesting aspects and a considerable amount of work was necessary in order to bring the final analytic result to a manageable form. The calculation of these 11 integrals is described in detail in [69]. In order to obtain the 7 color coefficients we are interested in, up to terms of  $\mathcal{O}(\varepsilon^0)$  included, the MIs need to be evaluated up to the order in  $\varepsilon$  where GHPLs of weight 4 appear.

Once the bare expression of the 7 color coefficients is available, one needs to carry out the UV renormalization. The renormalization procedure is standard. However, we provide some further details in Section 3.2.

### 3.2 Renormalization

As in our previous papers on two-loop corrections to top-quark pair production [37–39], we employ a mixed renormalization scheme in which the wave functions and the heavy-quark mass are renormalized on shell, while the strong coupling constant is renormalized in the  $\overline{\text{MS}}$  scheme. The explicit expressions of the one- and two-loop renormalized amplitudes in terms of bare functions and counterterms are explicitly provided in Eq. (4.6) of reference [39]. As explained in that work, the bare amplitudes as well as the relevant renormalization constants are expanded in powers of  $\alpha_s/\pi$ . The one-loop renormalization constants can be found in Eqs. (4.7-4.10) in [39]. Here, we just add the explicit expression of the two-loop renormalization constants needed to renormalize the  $N_l$ ,  $N_l N_h$  and  $N_l^2$  part of the two-loop matrix elements. By employing the notation in [39] one finds

$$\delta Z_{\text{WF},t}^{(2)} = C^2(\varepsilon) \left( \frac{\mu^2}{m^2} \right)^{2\varepsilon} C_F N_l T_R \left[ \frac{1}{8\varepsilon^2} + \frac{9}{16\varepsilon} + \frac{\zeta_2}{2} + \frac{59}{32} \right], \quad (3.1)$$

$$\delta Z_{\text{WFG}}^{(2)} = 0, \quad (3.2)$$

$$\delta Z_{\alpha_s}^{(2)} = C^2(\varepsilon) \left( \frac{e^{-\gamma\varepsilon}}{\Gamma(1+\varepsilon)} \right)^2 \frac{N_l T_R}{4\varepsilon} \left[ \left( \frac{8}{9} N_h T_R + \frac{4}{9} N_l T_R - \frac{22}{9} C_A \right) \frac{1}{\varepsilon} + \frac{5}{6} C_A + \frac{C_F}{2} \right], \quad (3.3)$$

$$\delta Z_m^{(2)} = C^2(\varepsilon) \left( \frac{\mu^2}{m^2} \right)^{2\varepsilon} N_l T_R \left[ \frac{1}{8\varepsilon^2} + \frac{7}{16\varepsilon} + \frac{\zeta_2}{2} + \frac{45}{32} + \left( \frac{279}{64} + \frac{7}{4}\zeta_2 + \zeta_3 \right) \varepsilon \right]. \quad (3.4)$$

As usual, in the QCD case with  $SU(N_c = 3)$  we have  $C_A = 3$ ,  $C_F = 4/3$  and  $T_R = 1/2$ . Finally,  $\gamma \approx 0.577216$  is the Euler-Mascheroni constant and  $C(\varepsilon) = (4\pi)^\varepsilon \Gamma(1+\varepsilon)$  is a factor which reabsorbs the logarithms of  $4\pi$  and  $\gamma$ -dependent terms in the  $\varepsilon$  expansion.

### 3.3 Multiple polylogarithms

Our results are obtained by inserting the appropriate MIs in the IBP reduction of each diagram. Consequently, the results share the analytical properties of the MIs, which have different branch cuts. The correct way of crossing the cuts is dictated by causality, which is enforced by the  $i\delta$  ( $\delta \rightarrow 0^+$ ) term in the Feynman propagators. The various MIs encountered in the present calculation can have thresholds located at  $s = 0$ ,  $s = 4m^2$ ,  $t = m^2$  and  $u = m^2$  (see the discussion in [69]). In the physical region one finds that  $s \geq 4m^2$  and that both  $t$  and  $u$  are negative. It is then sufficient to associate an infinitesimal positive imaginary part to  $s$  in order to have well defined results.

The color coefficients  $E_l$ ,  $F_l$ ,  $G_l$ ,  $H_l$ ,  $H_{lh}$ ,  $I_l$ , and  $I_{lh}$  depend on three independent variables: the top-quark mass  $m$  and two of the three dimensionless variables  $x$ ,  $y$  and  $z$ , where

$$x = -\frac{1 - \sqrt{1 - \frac{4m^2}{s}}}{1 + \sqrt{1 - \frac{4m^2}{s}}}, \quad y = -\frac{t}{m^2}, \quad z = -\frac{u}{m^2}. \quad (3.5)$$

The momentum conservation relation among Mandelstam invariants can be rewritten in terms of  $x$ ,  $y$  and  $z$  as follows:

$$y + z + \frac{1 + x^2}{x} = 0. \quad (3.6)$$

In the physical phase-space region, the following inequalities hold:

$$m^2 > 0, \quad -1 \leq x < 0, \quad -x \leq y \leq -\frac{1}{x}, \quad -x \leq z \leq -\frac{1}{x}, \quad yz \geq 1, \quad y + z \geq 2. \quad (3.7)$$

The color coefficients we are interested in can be written in terms of GHPLs of arguments  $x$ ,  $y$  and  $z$  up to weight four [69]. The GHPLs are defined through iterated integrations by the relations

$$G(w_1, w_2, \dots, w_n; q) \equiv \int_0^q dt \frac{1}{t - w_1} G(w_2, \dots, w_n; t),$$

$$G(\underbrace{0, \dots, 0}_n; q) \equiv \frac{1}{n!} \ln^n q. \quad (3.8)$$

The variable  $q$  can be  $x$ ,  $y$  or  $z$  and the weights  $w_i$  are simple rational functions of  $x$ ,  $y$ ,  $z$  or complex constants ( $w_i \in \mathbb{C}$ ).

For univariate multiple polylogarithms with argument  $q = x$ , it was found useful to generalize the definition of GHPLs by allowing polynomial denominators, as follows

$$G([f(o)], w_2, \dots, w_n; q) = \int_0^q dt \frac{f'(t)}{f(t)} G(w_2, \dots, w_n; t), \quad (3.9)$$

where  $f(o)$  is an irreducible rational polynomial of arbitrary degree and  $o$  is a dummy variable. Here, the weights are restricted to be independent of external variables. In the following, we will refer to the weights of the form  $[f(o)]$  as *generalized weights* [69, 103]. Since  $f(o)$  is a polynomial of degree  $n$ , one can always choose to normalize the coefficients in such a way that the cofactor of  $o^n$  is equal to 1. The polynomial  $f(o)$  can be written in terms of its  $n$  complex roots  $r_i$  as

$$f(t) = (t - r_1)(t - r_2) \cdots (t - r_n); \quad (3.10)$$

since

$$\frac{f'(t)}{f(t)} = \frac{1}{t - r_1} + \frac{1}{t - r_2} + \cdots + \frac{1}{t - r_n}, \quad (3.11)$$

a GHPL with generalized weights is related to GHPLs with constant complex weights  $r_i$

$$G(\cdots, [f(o)], \cdots; q) = G(\cdots, r_1, \cdots; q) + G(\cdots, r_2, \cdots; q) + \cdots + G(\cdots, r_n, \cdots; q). \quad (3.12)$$

In our case, the introduction of the GHPLs in Eq. (3.9) is indeed enough to handle all non-linear denominators in the integrating factors and no complex weights are needed. In particular, we employ a single GHPL with weight  $[f(o)] = [1 - o + o^2]$  instead of the corresponding pair of GHPLs with complex weights

$$r_{1,2} = -\frac{1}{2} \left( 1 \pm i\sqrt{3} \right), \quad (3.13)$$

using Eq. (3.12). Similarly, we encounter the generalized weight  $[f(o)] = [1 + o^2]$ , which is related to the pair of complex weights  $r_{1,2} = \pm i$ . Besides leading to more compact results, the generalized weights prevent the appearance of spurious imaginary parts present in each of the GHPLs with complex weights. The GHPLs of the kind in Eq. (3.9) can be evaluated numerically by means of the package described in [64], again by employing the relation in Eq. (3.12). A very important feature of the generalized weights resides in the fact that the corresponding integrating factors satisfy the relation

$$dt \frac{f'(t)}{f(t)} = d \ln(f(t)), \quad (3.14)$$

which allows for the construction of symbols and coproducts without reference to roots of irreducible polynomials (see [103] for details and [104, 105] for related extensions of multiple polylogarithms).

A large fraction of the work presented in this paper was devoted to simplify the color coefficients in terms of GHPLs, cast them into a representation suitable for numerical evaluation and expand them in different kinematical limits. Initially, the MIs are expressed in terms of different pairs of variables chosen in the set  $\{x, y, z\}$ . For a planar integral there is usually a “natural” choice for this pair (corresponding to the cut structure of the MI), which renders the expressions particularly compact. The situation is considerably more involved for non-planar integrals, where cuts in all three channels  $s$ ,  $t$  and  $u$  are present simultaneously. A naive substitution of the MIs in the expression of the cross section produces large analytic results which are difficult to manipulate. The difficulties are of



several kinds. First of all, the simultaneous presence of  $x$ ,  $y$  and  $z$  gives rise to redundancies in the representation of the color coefficients (i.e. the latter can contain hidden zeros), because of Eq. (3.6). This proliferation of terms makes the numerical evaluation of the color coefficients more time consuming. Moreover, it is a non-trivial task to extract the real and imaginary parts of the interference between two-loop and tree-level diagrams and to write it in terms of real-valued GHPLs. In fact, we encounter GHPLs which are real in some phase-space regions and complex in others. Finally, GHPLs of arguments  $x$ ,  $y$  and  $z$  are not straightforwardly expanded near the production threshold or in the asymptotic small-mass (or high-energy) limit. Our solution to these problems relies on the methods outlined below.

At first, we choose to rewrite the color coefficients by eliminating  $z$  in terms of  $x$  and  $y$ . Furthermore, for  $y$ -dependent GHPLs we choose  $y$  as the GHPL argument (resulting in  $x$ -dependent or constant weights), while for  $y$ -independent GHPLs we choose  $x$  as argument (resulting in generalized or constant weights). Involved substitutions are necessary in order to recast the GHPLs depending on  $\{z, x\}$  or  $\{y, z\}$  in terms GHPLs depending on  $\{y, x\}$ . These transformations as well as others needed for the expansions in the kinematic limits discussed in Section 5 are generated by means of `GPLChangeArg` [106], a new automated argument-change algorithm written in `Mathematica`. The algorithm does not involve the use of the symbol or the coproduct and matches constants using high precision numerical evaluations of GHPLs [64].

It turns out that the color coefficients are faster to evaluate and numerically more stable when we insist on the use of specific types of multiple polylogarithms rather than on specific ways in which the kinematic invariants  $x$  and  $y$  enter in the argument and weights of the transcendental functions. For this reason, we rewrite our results in a second normal form. In this case, instead of GHPLs of arguments  $x$  and  $y$ , we choose to employ the functions  $\ln$ ,  $\text{Li}_n$  ( $n = 2, 3, 4$ ) and  $\text{Li}_{2,2}$ , where the arguments are (complicated) rational functions of  $x$  and  $y$ . In particular, we choose the arguments such that the functions are real valued everywhere in the physical region of phase space. The  $\text{Li}_{m_1, \dots, m_k}$  functions ( $m_i \in \mathbb{N}$ ) can be represented in terms of nested sums

$$\text{Li}_{m_1, \dots, m_k}(x_1, \dots, x_k) = \sum_{i_k=1}^{\infty} \frac{x_k^{i_k}}{i_k^{m_k}} \sum_{i_{k-1}=1}^{i_k-1} \frac{x_{k-1}^{i_{k-1}}}{i_{k-1}^{m_{k-1}}} \cdots \sum_{i_1=1}^{i_2-1} \frac{x_1^{i_1}}{i_1^{m_1}}, \quad (3.15)$$

for  $|x_1 \cdots x_j| \leq 1$  for all  $j \in \{1, \dots, k\}$  and  $(m_1, x_1) \neq (1, 1)$ . In general, Li functions and GHPLs are related by

$$\text{Li}_{m_1, \dots, m_k}(x_1, \dots, x_k) = (-1)^k G\left(\underbrace{0, \dots, 0, \frac{1}{x_k}}_{m_k}, \dots, \underbrace{0, \dots, 0, \frac{1}{x_1 \cdots x_k}}_{m_1}\right) \quad (3.16)$$

and thus describe the same set of functions. In particular, they can be evaluated numerically with the same tools employed for GHPLs [64]. Explicitly, we have

$$\text{Li}_n(x) = -G\left(\underbrace{0, \dots, 0, 1}_n; x\right), \quad \text{Li}_{2,2}(x_1, x_2) = G\left(0, \frac{1}{x_1}, 0, \frac{1}{x_1 x_2}; 1\right). \quad (3.17)$$

for the functions considered here. The translation to the new functional basis is carried out by employing another automated algorithm implemented in `Mathematica: GPLReduce` [106]. The latter is an improved coproduct based normal form algorithm, and it extends the procedure outlined in [74] to the case of GHPLs depending on generalized weights. The algorithm determines algebraic constants from numerical samples of GHPLs obtained with [64]. It is indeed interesting to observe that algorithms based on coproduct apply also to the case of the generalized weights introduced in Eq. (3.9).

## 4 Analytic results

In this section we present our results. By using the techniques described in Section 3.3, we can write closed analytic expressions for the UV renormalized color coefficients  $E_l$ ,  $F_l$ ,  $G_l$ ,  $H_l$ ,  $H_{lh}$ ,  $I_l$ , and  $I_{lh}$  in Eq. (2.5). These expressions are valid for arbitrary values of the top-quark mass and of the Mandelstam invariants. Furthermore, as mentioned in the previous section, they are at first derived by writing all the GHPLs in terms of the dimensionless variables  $x$  and  $y$  (we remind the reader that  $x < 0$  in the physical region). In the case of GHPLs of two variables, we always choose  $y$  as the functional argument. Correspondingly, the weights of the GHPLs of argument  $y$  are part of the set

$$\left\{ -1, 0, -\frac{1}{x}, -x, -\frac{(1+x^2)}{x}, -\frac{(1-x+x^2)}{x} \right\}. \quad (4.1)$$

The GHPLs of argument  $x$  have weights

$$\{-1, 0, 1, [1+o^2], [1-o+o^2]\}. \quad (4.2)$$

The maximum transcendentality of the GHPLs present in our results is 4. The total number of GHPLs is 289 if we expand all GHPLs products; by exploiting the shuffle algebra we reduced this number to 221 independent GHPLs. It is interesting to observe that in the color coefficients  $E_l$ ,  $F_l$ , and  $G_l$  the transcendentality of the GHPLs present in the finite part is 4, while the single pole part involves only GHPLs of transcendentality 2. The analytic expressions are lengthy and can be found in the ancillary file `ggtt-lightnf-argyx.m` attached to the arXiv submission of this article.

As discussed in Section 3.3, the numerical evaluation speed and stability of the results benefit from writing the analytic color coefficients in terms of specific real valued Li functions, where the arguments are (complicated) rational functions of  $x$  and  $y$ . With this choice, the imaginary parts of the tree-level times two-loop interferences appear explicitly multiplied by a factor  $i\pi$  and it is therefore trivial to extract the real part of that result, which coincides up to a factor of 2 with the color coefficients we are interested in. The total number of independent multiple polylogarithms we employ for the seven color coefficients is 225. Only 57 of these are  $\text{Li}_{2,2}$ , while the others are logarithms and classical polylogarithms  $\text{Li}_n$  ( $n = 2, 3, 4$ ). Examples for the Li functions' arguments are

$$\pm x, \pm x^2, -\frac{1}{y}, -y, -\frac{y}{x}, -x(x+y), \frac{x+y}{y}, -\frac{x+z(x,y)}{x+y}, \dots$$

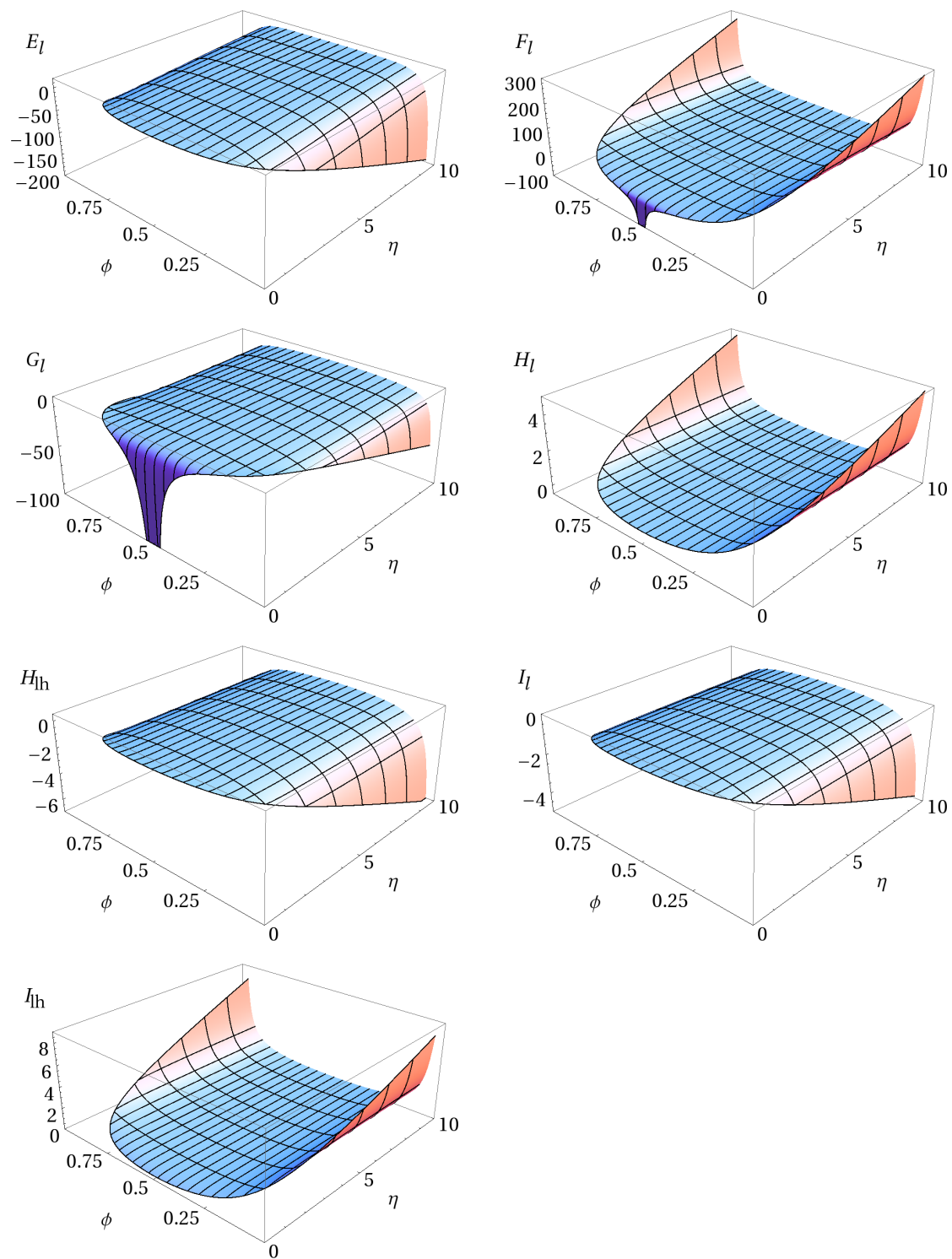


**Figure 2.** Finite parts of the color coefficients as functions of  $\eta = s/(4m^2) - 1$  and  $\phi = -(t - m^2)/s$ . The finite parts plotted here are normalized in the standard  $\overline{\text{MS}}$  way (see Appendix A). The renormalization scale  $\mu$  is set equal to the top quark mass.

Note that, although the total number of independent functions is not reduced by employing this representation instead of the one based on GHPLs of simple arguments, the numerical evaluation of the color coefficients is a factor of  $\sim 10$ -15 faster for typical phase space points. We conclude this is due to the simpler functional structure of the remaining multiple logarithms. When written in terms of Li functions, the seven color coefficients can be evaluated numerically in a generic phase-space point in a time of  $\mathcal{O}(1s)$ . For these numerical evaluations, we employed one 3.4 GHz core, double precision accuracy, `Mathematica` for the evaluation of  $\ln$  and  $\text{Li}_n$  functions and [64] for the evaluation of  $\text{Li}_{2,2}$  functions.

We emphasize that for our representation of the seven color coefficients in terms of Li functions, no new symbol letters were introduced beyond the ones that follow from Eqs. (4.1) and (4.2). We observe that all of the generalized weights  $[f(o)]$  introduced in Eq. (3.9) could be eliminated from the result with the new choice of basis functions. Specifically, the functions depending on the generalized weights appear in the color coefficients only in particular combinations with other multivariate polylogarithms. These combinations can be rewritten in terms of normal GHPLs of rational weights.

Also in the case in which one employs Li functions, the complete analytic results are lengthy. We provide them via the ancillary file `ggtt-lightnf.m` attached to the arXiv submission of this work. Finally, following what was done in [38, 39], in Fig. 2 we plot the finite part of the color coefficients as a function of the variables  $\eta$  and  $\phi$ , defined as

$$\eta = \frac{s}{4m^2} - 1, \quad \phi = -\frac{t - m^2}{s}, \quad \text{where } \frac{1}{2} \left( 1 - \sqrt{\frac{\eta}{1 + \eta}} \right) \leq \phi \leq \frac{1}{2} \left( 1 + \sqrt{\frac{\eta}{1 + \eta}} \right). \quad (4.3)$$

In addition, we give numerical values for three benchmark points in Appendix A.

We performed several checks of our results. The IR poles of  $E_l, F_l, G_l, H_l, H_{lh}, I_l$ , and  $I_{lh}$  were first derived in [107]. We found full analytical agreement between the IR poles we obtained and the results available in the literature. In order to test the finite parts of the seven color coefficients, we compared them with the numerical results presented in Table 4.2 of [108], that are valid for  $s/m^2 = 5$ ,  $t/m^2 = -1.25$ , and  $\mu/m = 1$ . After accounting for the different normalization, we found complete agreement on all of the 10 significant digits provided in that table.

## 5 Expansions

One of the advantages of working with analytic expressions resides in the fact that one can readily obtain useful expansions of the results in particularly interesting phase-space regions. Here, we consider two different expansions: the expansion near the production threshold  $s \sim 4m^2$ , and the expansion in the small-mass (high-energy) limit  $s \gg m^2$ .

### 5.1 Threshold expansion

The threshold region is identified by taking the limit  $\beta \rightarrow 0$ , where  $\beta$  is the top-quark velocity in the  $t\bar{t}$  rest frame,

$$\beta \equiv \sqrt{1 - \frac{4m^2}{s}}, \quad (5.1)$$

at fixed scattering angle  $\theta$ . The first few orders of the expansion of the color coefficients take the following remarkably simple form

$$\begin{aligned}
E_l = & -\frac{7}{12\varepsilon^3} - \frac{1}{\varepsilon^2} \left( \frac{L_\mu}{2} - \ln 2 - \frac{5}{12} \right) + \frac{1}{216\varepsilon} (-36L_\mu^2 + 144L_\mu \ln 2 + 348L_\mu - 144 \ln^2 2 \\
& - 696 \ln 2 + 252\zeta_2 + 761) + \frac{1}{648} (504L_\mu^2 - 2016L_\mu \ln 2 + 216L_\mu\zeta_2 - 456L_\mu \\
& + 2016 \ln^2 2 - 432\zeta_2 \ln 2 + 1884 \ln 2 - 2430\zeta_2 - 414\zeta_3 - 3185) \\
& + \beta^2 \left[ -\frac{7}{12\varepsilon^3} (c_\theta^2 + 2) + \frac{1}{12\varepsilon^2} (-6L_\mu c_\theta^2 - 12L_\mu + 12 \ln 2 c_\theta^2 + 24 \ln 2 + 16c_\theta^2 - 23) \right. \\
& + \frac{1}{216\varepsilon} (-36L_\mu^2 c_\theta^2 - 72L_\mu^2 + 144L_\mu c_\theta^2 \ln 2 + 288L_\mu \ln 2 + 528L_\mu c_\theta^2 + 156L_\mu \\
& - 144c_\theta^2 \ln^2 2 - 288 \ln^2 2 - 1824c_\theta^2 \ln 2 + 24 \ln 2 + 252c_\theta^2 \zeta_2 + 2513c_\theta^2 + 504\zeta_2 \\
& - 326) + \frac{1}{648} (720L_\mu^2 c_\theta^2 + 360L_\mu^2 - 2880L_\mu c_\theta^2 \ln 2 - 1440L_\mu \ln 2 + 216L_\mu c_\theta^2 \zeta_2 \\
& + 228L_\mu c_\theta^2 + 432L_\mu \zeta_2 - 696L_\mu + 3456c_\theta^2 \ln^2 2 + 864 \ln^2 2 + 10422c_\theta^2 \zeta_2 \ln 2 \\
& + 24312c_\theta^2 \ln 2 - 8316\zeta_2 \ln 2 - 11712 \ln 2 - 10476c_\theta^2 \zeta_2 - 9459c_\theta^2 \zeta_3 - 12200c_\theta^2 \\
& \left. + 4158\zeta_2 + 5382\zeta_3 + 2576) \right] + \mathcal{O}(\beta^4), \tag{5.2}
\end{aligned}$$

$$\begin{aligned}
F_l = & \frac{1}{\beta} \left[ \frac{\zeta_2}{2\varepsilon} - \frac{7\zeta_2}{3} \right] + \frac{7}{6\varepsilon^3} + \frac{1}{\varepsilon^2} \left( L_\mu - 2 \ln 2 - \frac{1}{3} \right) + \frac{1}{216\varepsilon} (72L_\mu^2 - 288L_\mu \ln 2 \\
& - 624L_\mu + 288 \ln^2 2 + 1248 \ln 2 - 450\zeta_2 - 1897) + \frac{1}{648} (-1008L_\mu^2 + 4032L_\mu \ln 2 \\
& - 432L_\mu \zeta_2 - 96L_\mu - 4032 \ln^2 2 + 864\zeta_2 \ln 2 - 4128 \ln 2 + 5103\zeta_2 + 693\zeta_3 + 7339) \\
& + \beta \left[ \frac{1}{\varepsilon} \left( \frac{3\zeta_2}{2} - \frac{c_\theta^2 \zeta_2}{2} \right) - \frac{c_\theta^2 \zeta_2}{6} - 4\zeta_2 \right] + \mathcal{O}(\beta^2), \tag{5.3}
\end{aligned}$$

$$\begin{aligned}
G_l = & \frac{1}{\beta} \left[ \frac{\zeta_2}{\varepsilon} - \frac{14\zeta_2}{3} \right] + \frac{1}{\varepsilon} \left( \frac{\zeta_2}{2} - \frac{17}{12} \right) + \frac{1}{36} (216\zeta_2 \ln 2 + 480 \ln 2 - 273\zeta_2 - 6\zeta_3 + 211) \\
& + \beta \left[ \frac{3\zeta_2}{\varepsilon} - 4c_\theta^2 \zeta_2 - 8\zeta_2 \right] + \mathcal{O}(\beta^2), \tag{5.4}
\end{aligned}$$

$$\begin{aligned}
H_l = & \frac{1}{9\varepsilon^2} - \frac{1}{3\varepsilon} + \frac{1}{9} (2 - \zeta_2) + \beta^2 \left[ \frac{1}{9\varepsilon^2} (c_\theta^2 + 2) - \frac{13}{18\varepsilon} c_\theta^2 - \frac{1}{18} (2c_\theta^2 \zeta_2 - 9c_\theta^2 + 4\zeta_2) \right] \\
& + \mathcal{O}(\beta^4), \tag{5.5}
\end{aligned}$$

$$\begin{aligned}
H_{lh} = & -\frac{2L_\mu}{9\varepsilon} + \frac{1}{9} (-L_\mu^2 + 6L_\mu - \zeta_2) + \beta^2 \left[ \frac{1}{36\varepsilon} (14c_\theta^2 - 8L_\mu c_\theta^2 - 16L_\mu - 9c_\theta^2 \zeta_2) \right. \\
& - \frac{1}{108} (12L_\mu^2 c_\theta^2 + 24L_\mu^2 - 156L_\mu c_\theta^2 + 54c_\theta^2 \zeta_2 \ln 2 - 84c_\theta^2 \ln 2 - 33c_\theta^2 \zeta_2 + 63c_\theta^2 \zeta_3 \\
& \left. + 10c_\theta^2 + 24\zeta_2) \right] + \mathcal{O}(\beta^4), \tag{5.6}
\end{aligned}$$

$$I_l = -\frac{2}{9\varepsilon^2} + \frac{2}{3\varepsilon} + \frac{2}{9} (\zeta_2 - 2) + \beta^2 \left[ -\frac{4}{9\varepsilon^2} + \frac{8}{9\varepsilon} c_\theta^2 - \frac{4}{9} (c_\theta^2 - \zeta_2) \right] + \mathcal{O}(\beta^4), \tag{5.7}$$

$$I_{lh} = \frac{4}{9\varepsilon} L_\mu + \frac{2}{9} (\zeta_2 - 6L_\mu + L_\mu^2) + \beta^2 \left[ \frac{8L_\mu}{9\varepsilon} + \frac{4}{9} (\zeta_2 - 4L_\mu c_\theta^2 + L_\mu^2) \right] + \mathcal{O}(\beta^4), \tag{5.8}$$

where  $L_\mu = \ln(\mu^2/m^2)$  and  $c_\theta \equiv \cos \theta$ . The threshold expansion up to and including terms of  $\mathcal{O}(\beta^5)$  can be found in the ancillary file `ggtt-lightnf-smallbeta.m`, which is included in the arXiv submission of this work. A comparison between exact results and threshold expansions at different orders in  $\beta$  is shown in Fig. 3. In the figure we set  $\cos \theta = 0.7$  and  $\mu = m$ .

In order to obtain the expansions in Eqs. (5.2-5.8), we start from the color coefficients written in terms of GHPLs depending on  $x$  and  $y$ . Subsequently, we rewrite each of the GHPLs of arguments  $\{y, x\}$  in terms of GHPLs of arguments  $\{\beta, \xi\}$ , where  $\xi = (1 - c_\theta)/2$ . We obtain GHPLs of argument  $\beta$  and weights included in the set

$$\left\{ -1, 0, 1, \frac{1}{1-2\xi}, -\frac{1}{1-2\xi}, [1+o^2], [3+o^2], [1+2o(1-2\xi)+o^2], [1-2o(1-2\xi)+o^2] \right\},$$

as well as HPLs of argument  $\xi$  and weights  $\{0, 1\}$ . (The  $\xi$  dependence of the generalized weights is beyond the scope for which we introduced this extension in Section 3.3; this is not an issue here since we do not consider variations of these GHPLs with respect to  $\xi$  nor do we employ symbols calculus for them.) The translation of the GHPLs from the  $\{y, x\}$  to the  $\{\beta, \xi\}$  basis involves a relatively large number of irrational constants related to logarithms and  $\text{Li}_n$  of fixed argument, as well as constants which are obtained from GHPLs of weights  $\{-2, -1, 0, 1, 2, [1+o^2], [1+o+o^2]\}$  and argument 1. These GHPLs of argument 1 can be rewritten in terms of the irrational constants. In some cases the relations can be easily found. For example:

$$\begin{aligned} G([1+o^2]; 1) &= \ln 2, & G([1+o+o^2]; 1) &= \ln 3, \\ G(0, [1+o^2]; 1) &= \frac{\pi^2}{24}, & G(0, [1+o+o^2]; 1) &= \frac{\pi^2}{9}. \end{aligned} \quad (5.9)$$

However, for GHPLs of higher weights these relations are difficult to find starting from the integral representation of the GHPLs. Consequently, relations of the type shown in Eq. (5.9) were found by means of numerical fitting routines working with a precision up to  $\sim 1000$  digits.

The GHPLs of argument  $\beta$  were then expanded in the limit  $\beta \rightarrow 0$ . The expansions of the individual GHPLs involve powers of  $\beta$  and  $\ln \beta$ , HPLs of argument  $\xi$  and weights  $\{0, 1\}$ , as well as the constants mentioned above. When the expansions of the individual GHPLs are inserted in the color coefficients, the  $\ln \beta$  as well as the HPLs of argument  $\xi$  cancel out. The same cancellation was observed already in the analogous expansion of the result in [39]. The expanded results depend only on powers of  $\beta$  (starting, in the case of the color coefficients  $F_l$  and  $G_l$ , from the power  $-1$ , which characterizes Coulomb singularities) and on powers of  $c_\theta^2$ . The forward-backward symmetry of the result is manifest. It is also striking to observe that the many irrational constants appearing in the expansion of the individual GHPLs combine in such a way that in the expansion of the color coefficients only the constants  $\zeta_2$ ,  $\zeta_3$  and  $\ln 2$  are present.

## 5.2 Small mass expansion

In this Section we discuss the expansion of our results in the small-mass (or high-energy) limit, defined as the region where  $s, |t|, |u| \gg m^2$ . It must be noted that the two-loop

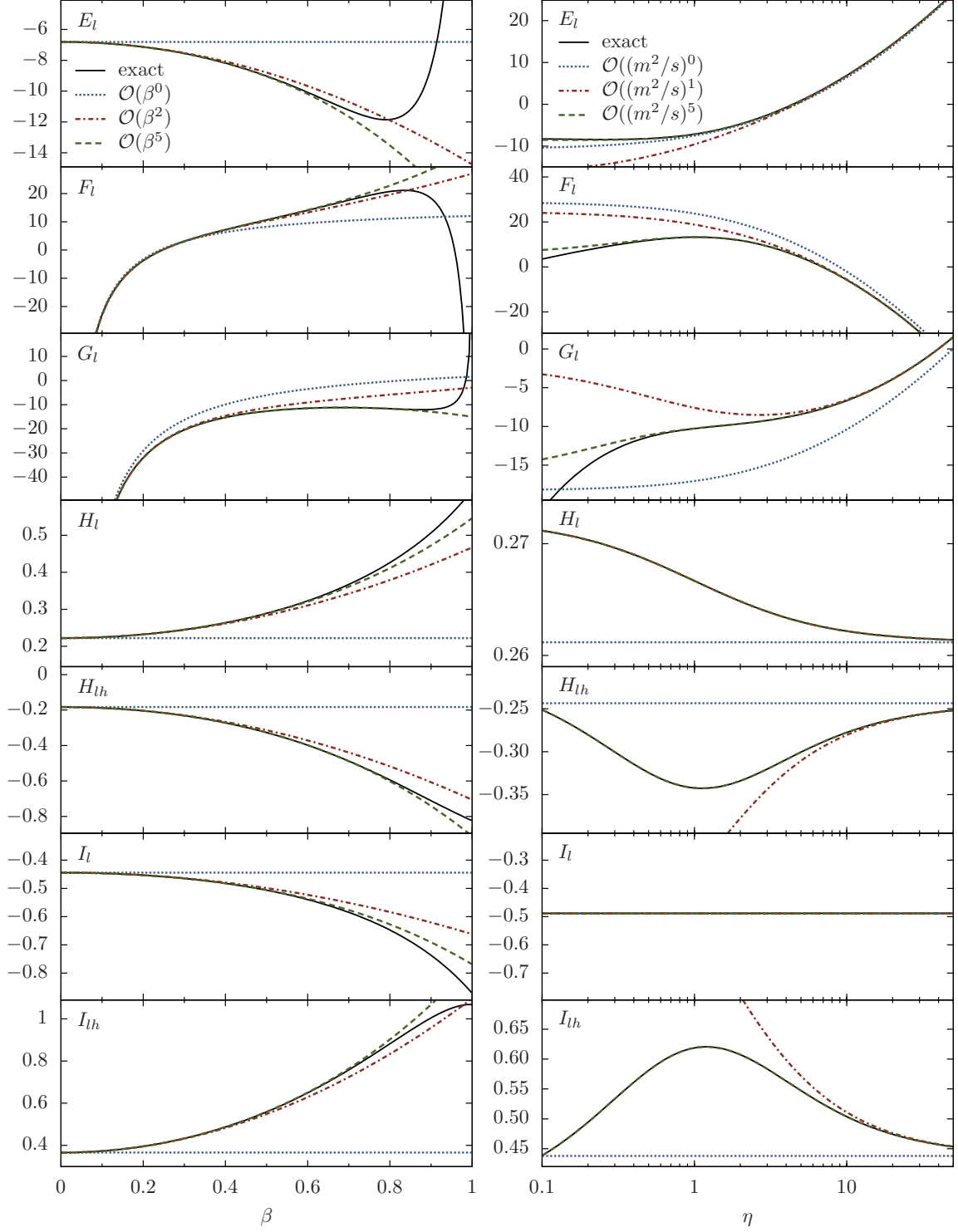


**Figure 3.** Left column: finite parts of the color coefficients as a function of  $\beta = \sqrt{1 - 4m^2/s}$  for  $\cos\theta = 0.7$ . Right column: the same, but in the high energy region as a function of  $\eta = s/(4m^2) - 1$  for  $\phi = -(t - m^2)/s = 0.35$ . We set  $\mu = m$  and employ  $\overline{\text{MS}}$  normalization (see Appendix A).

corrections to the top-quark pair production at leading order in this limit were calculated a few years ago [35, 36]. We can therefore test our calculation by comparing the leading order of the expansions we present here with the results available in the literature.

The expansions are parametrized by the ratio  $m^2/s \rightarrow 0$ , where the dimensionless parameter  $\phi = -(t - m^2)/s$  is kept fixed. The expansions of the seven color coefficients in the  $m^2/s \rightarrow 0$  limit up to and including terms of  $\mathcal{O}((m^2/s)^5)$  can be found in the ancillary file `ggtt-lightnf-smallmass.m` included in the arXiv submission of this work. The leading terms in these expansions fully agree with the corresponding results in [36], provided that one accounts for the difference in the overall normalization factor. For this reason, we do not type these results here. The right column in Fig. 3 compares the exact results for the color coefficients with the small mass expansions obtained by retaining terms of  $\mathcal{O}((m^2/s)^0)$ ,  $\mathcal{O}(m^2/s)$  and  $\mathcal{O}((m^2/s)^5)$ . In those plots we set  $\phi = 0.35$  and  $\mu = m$ . As expected, for large values of  $\eta$ , all of the expansions reproduce the exact result.

In order to obtain expansions in the small mass limit, it is convenient to first rewrite the color coefficients in terms of GHPLs of arguments  $\{x, \phi\}$ . (Note that the more obvious choice  $\{m^2/s, \phi\}$  requires the introduction of square root factors which make subsequent algebraic manipulations inconvenient.) The color coefficient can be written in terms of GHPLs of argument  $x$  and weights belonging to the set

$$\left\{ -1, 0, 1, -\frac{1-\phi}{\phi}, -\frac{\phi}{1-\phi}, [1+o^2], [1-o+o^2], \left[1+o\frac{1-2\phi}{\phi}+o^2\right], \left[1-o\frac{1-2\phi}{1-\phi}+o^2\right] \right\},$$

together with HPLs of argument  $\phi$  and weights  $\{0, 1\}$ . The only transcendental constants involved are powers of  $\pi$  and  $\zeta_3$ . The expansion of the GHPLs of argument  $x$  can be carried out by first expanding them in the  $x \rightarrow 0$  limit and then by expanding  $x$  in powers of  $m^2/s$ :

$$x = -\frac{m^2}{s} - 2\left(\frac{m^2}{s}\right)^2 - 5\left(\frac{m^2}{s}\right)^3 - 14\left(\frac{m^2}{s}\right)^4 + \dots \quad (5.10)$$

The expansion of these GHPLs in  $m^2/s$  involves logarithms of the same ratio, HPLs of argument  $\phi$  and irrational constants which depend on  $\zeta_3$  and powers of  $\pi$ . We insert the expansions of the GHPLs of argument  $x$  in the color coefficients and rewrite the HPLs of argument  $\phi$  and weights  $\{0, 1\}$  in yet another form. Here, it is sufficient to choose logarithms and  $\text{Li}_n$  ( $n = 2, 3, 4$ ) of arguments  $\phi$  and  $1 - \phi$ , as well as

$$\text{Li}_4\left(-\frac{\phi}{1-\phi}\right), \quad \text{Li}_4\left(-\frac{1-\phi}{\phi}\right).$$

In order to have the invariance of the result under the transformation  $\phi \rightarrow 1 - \phi$  (forward-backward symmetry) manifest, we arrange for a functional basis such that the functions listed above enter in the combinations  $(f(\phi) + f(1 - \phi))$  or  $((2\phi - 1)(f(\phi) - f(1 - \phi)))$ . The cofactors of these building blocks depend on  $\phi$  only through powers of  $(2\phi - 1)^2 - 1$ ; spurious poles at  $\phi = 1/2$  which appear at intermediate stages cancel out. At this point, the final results for the expansions are manifestly forward-backward symmetric and numerically stable.



## 6 Conclusions

In this paper we obtained analytic expressions for all of the two-loop corrections with a closed light-quark loop which contribute to top-quark pair production in the gluon-fusion channel. The calculation is carried out by retaining the full dependence on the top-quark mass. The two-loop diagrams are interfered with the tree-level diagrams, and the results are presented as analytic formulas for the corresponding seven gauge-independent color coefficients in the NNLO virtual contributions proportional to the number of light quarks  $N_l$  (see Eq. (2.5)). The analytic results are collected in ancillary files included in the arXiv submission of this work. For illustrative purposes, we present plots of the finite parts of the color coefficients as functions of the dimensionless parameters  $\eta$  and  $\phi$ , and we provide numerical values at three different benchmark points in the physical phase space. Furthermore, in this work it was shown that, after the results are written in a suitable form, expansions in the production threshold and small mass limits can be obtained in a straightforward manner. The expanded color coefficients in both limits are also provided in ancillary files included in the arXiv submission of this work.

In comparison to analytic results for the two-loop corrections involving a closed quark loop in the quark annihilation channel [37] and for corrections contributing to the leading color coefficient in both channels [38, 39], the results discussed in the present work have a more involved structure. The number of GHPLs and the kind of weights which arise in the calculation of the box MIs [69] made it mandatory to devote a large amount of work to the efficient organization and simplification of the final result. This required numerous non-trivial rewritings of the color coefficients using different sets of functional bases depending on different pairs of dimensionless variables, as well as a mapping of the GHPLs to real valued functions specifically suitable for fast and stable numerical evaluations.

In particular, we show that the exact results for the color coefficients can be expressed in terms of logarithms, classical polylogarithms  $\text{Li}_n$  ( $n = 2, 3, 4$ ), and genuine multiple polylogarithms  $\text{Li}_{2,2}$ . Here, the functional arguments are chosen such that the functions are real valued over the entire physical phase space. This change in the functional basis was made possible by an extension of the algorithms given in [74, 76] suitable to handle GHPLs depending on the generalized weights employed for non-linear denominators in the integrating factors in this work. For the first time, we demonstrated that such a basis choice is possible also in the presence of generalized weights for a multiscale QCD application. We emphasize that no spurious symbol letters needed to be introduced and all generalized weights could be eliminated. We observe that the numerical evaluation of the color coefficients is faster by an order of magnitude when this optimized functional basis is employed.

It will be interesting to see if the methods developed and employed for the results presented here can be applied to the calculation of the subleading two-loop color coefficients in the quark-annihilation channel. These subleading color coefficients involve a number of non-planar diagrams with massive internal and external particles and to date they were calculated only numerically [5]. In the gluon-fusion channel, the subleading color coefficients  $B, C, D$  and the heavy-quark contributions  $E_h, F_h, G_h$  are known only numerically

[108]. The analytic calculation of these gluon initiated corrections poses an additional independent challenge, since they are known to depend on MIs which involve elliptic integrals. Those structures arise from diagrams which include a sunrise subtopology with three massive internal legs and a momentum transferred which is not on the mass shell of the internal legs [109]. Recent developments [110, 111] give rise to the hope that a better understanding of the analytic structure of massive Feynman diagrams will also allow for an analytic evaluation of these sets of corrections.

## Acknowledgments

Part of the algebraic manipulations required in this work were carried out with FORM [112]. The Feynman diagrams were drawn with Axodraw [113]. The work of AvM was supported in part by the Schweizer Nationalfonds (Grant 200020\_124773/1), by the Research Center *Elementary Forces and Mathematical Foundations (EMG)* of the Johannes Gutenberg University of Mainz and by the German Research Foundation (DFG). The work of AF was supported in part by the PSC-CUNY Award No. 66590-00-44 and by the National Science Foundation Grant No. PHY-1068317. The work of RB was supported by European Community Seventh Framework Programme FP7/2007-2013, under grant agreement N.302997.

## A Numerical samples

In this appendix, we present numerical results for all of the seven color coefficients we calculated. Each one of the following tables shows values of the pole coefficients and finite parts for a different benchmark point in the physical phase space. The results shown here are normalized in the standard  $\overline{\text{MS}}$  way, that is a factor  $((4\pi)^\epsilon e^{-\gamma\epsilon})^2$  is extracted and not included in the numerics. That means that the results in the ancillary files are first multiplied by a factor  $e^{2\gamma\epsilon}\Gamma^2(1+\epsilon)$  and then expanded in  $\epsilon$  before the numbers are obtained.

For  $s/m^2 = 5$ ,  $t/m^2 = -1.25$ ,  $\mu/m = 1$  we obtain

Coeff.	$1/\epsilon^3$	$1/\epsilon^2$	$1/\epsilon$	$\epsilon^0$
$E_l$	-0.7838122811	1.137904118	1.747317683	-7.037881174
$F_l$	1.552103527	-1.663042888	-3.172113037	7.815862217
$G_l$	-	0.1937203624	4.190187785	-13.38175914
$H_l$	-	0.1492975773	-0.3407519641	0.2270538721
$H_{lh}$	-	-	-0.0002689061861	-0.2466070280
$I_l$	-	-0.2956387670	0.6756453423	-0.4489337823
$I_{lh}$	-	-	-	0.4863062794

For  $s/m^2 = 43$ ,  $t/m^2 = -21$ ,  $\mu/m = 1.7$  we obtain

Coeff.	$1/\varepsilon^3$	$1/\varepsilon^2$	$1/\varepsilon$	$\varepsilon^0$
$E_l$	-0.6828131172	2.465864806	-2.816012729	-2.086232939
$F_l$	1.364888058	-4.939937930	4.260219926	11.41745753
$G_l$	-	1.589549879	-3.010243755	-10.88329499
$H_l$	-	0.1300596414	-0.3337514448	0.2224382692
$H_{lh}$	-	-	-0.2760509183	0.3479512918
$I_l$	-	-0.2599786777	0.6671476671	-0.4446849447
$I_{lh}$	-	-	0.5518081243	-0.6955768357

For  $s/m^2 = 8.1$ ,  $t/m^2 = -0.6$ ,  $\mu/m = 2.1$  we obtain

Coeff.	$1/\varepsilon^3$	$1/\varepsilon^2$	$1/\varepsilon$	$\varepsilon^0$
$E_l$	-1.991067909	-0.1771655934	12.03682866	-24.21746110
$F_l$	2.915285996	-0.07400739283	-17.47415387	35.65735116
$G_l$	-	1.105009458	3.962101090	-15.96447616
$H_l$	-	0.3792510302	-0.7898719870	0.4900775204
$H_{lh}$	-	-	-1.131777182	0.8530176592
$I_l$	-	-0.5552925707	1.179700855	-0.7009615385
$I_{lh}$	-	-	1.647969182	-1.364946933

## References

- [1] P. Baernreuther, M. Czakon, and A. Mitov, *Percent Level Precision Physics at the Tevatron: First Genuine NNLO QCD Corrections to  $q\bar{q} \rightarrow t\bar{t} + X$* , Phys. Rev. Lett. **109** (2012) 132001 [[arXiv:1204.5201](#)].
- [2] M. Czakon and A. Mitov, *NNLO corrections to top-pair production at hadron colliders: the all-fermionic scattering channels*, JHEP **1212** (2012) 054 [[arXiv:1207.0236](#)].
- [3] M. Czakon and A. Mitov, *NNLO corrections to top pair production at hadron colliders: the quark-gluon reaction*, JHEP **1301** (2013) 080 [[arXiv:1210.6832](#)].
- [4] M. Czakon, P. Fiedler, and A. Mitov, *The total top quark pair production cross-section at hadron colliders through  $O(\alpha_s^4)$* , Phys. Rev. Lett. **110** (2013) 252004 [[arXiv:1303.6254](#)].
- [5] M. Czakon, *Tops from Light Quarks: Full Mass Dependence at Two-Loops in QCD*, Phys. Lett. B **664**, 307 (2008) [[arXiv:0803.1400](#)].
- [6] M. Czakon, *A novel subtraction scheme for double-real radiation at NNLO*, Phys. Lett. B **693** (2010) 259 [[arXiv:1005.0274](#)].
- [7] M. Czakon, *Double-real radiation in hadronic top quark pair production as a proof of a certain concept*, Nucl. Phys. B **849** (2011) 250 [[arXiv:1101.0642](#)].
- [8] S. Dittmaier, P. Uwer, and S. Weinzierl, *NLO QCD corrections to  $t$  anti- $t$  + jet production at hadron colliders*, Phys. Rev. Lett. **98** (2007) 262002 [[hep-ph/0703120](#)].
- [9] S. Dittmaier, P. Uwer, and S. Weinzierl, *Hadronic top-quark pair production in association with a hard jet at next-to-leading order QCD: Phenomenological studies for the Tevatron and the LHC*, Eur. Phys. J. C **59** (2009) 625 [[arXiv:0810.0452](#)].

- [10] G. Bevilacqua, M. Czakon, C. G. Papadopoulos, and M. Worek, *Dominant QCD Backgrounds in Higgs Boson Analyses at the LHC: A Study of  $pp \rightarrow t\bar{t} + 2$  jets at Next-To-Leading Order*, Phys. Rev. Lett. **104** (2010) 162002 [[arXiv:1002.4009](#)].
- [11] G. Bevilacqua, M. Czakon, C. G. Papadopoulos, and M. Worek, *Hadronic top-quark pair production in association with two jets at Next-to-Leading Order QCD*, Phys. Rev. D **84** (2011) 114017 [[arXiv:1108.2851](#)].
- [12] K. Melnikov and M. Schulze, *NLO QCD corrections to top quark pair production in association with one hard jet at hadron colliders*, Nucl. Phys. **B840** (2010) 129-159 [[arXiv:1004.3284](#)].
- [13] D. A. Kosower, *Antenna factorization of gauge theory amplitudes*, Phys. Rev. D **57** (1998) 5410 [[hep-ph/9710213](#)].
- [14] A. Gehrmann-De Ridder, T. Gehrmann, and E. W. N. Glover, *Antenna subtraction at NNLO*, JHEP **0509** (2005) 056 [[hep-ph/0505111](#)].
- [15] A. Daleo, T. Gehrmann, and D. Maitre, *Antenna subtraction with hadronic initial states*, JHEP **0704** (2007) 016 [[hep-ph/0612257](#)].
- [16] A. Daleo, A. Gehrmann-De Ridder, T. Gehrmann, and G. Luisoni, *Antenna subtraction at NNLO with hadronic initial states: initial-final configurations*, JHEP **1001** (2010) 118 [[arXiv:0912.0374](#)].
- [17] E. W. Nigel Glover and J. Pires, *Antenna subtraction for gluon scattering at NNLO*, JHEP **1006** (2010) 096 [[arXiv:1003.2824](#)].
- [18] R. Boughezal, A. Gehrmann-De Ridder, and M. Ritzmann, *Antenna subtraction at NNLO with hadronic initial states: double real radiation for initial-initial configurations with two quark flavours*, JHEP **1102** (2011) 098 [[arXiv:1011.6631](#)].
- [19] A. Gehrmann-De Ridder, T. Gehrmann and M. Ritzmann, *Antenna subtraction at NNLO with hadronic initial states: double real initial-initial configurations*, JHEP **1210** (2012) 047 [[arXiv:1207.5779](#)].
- [20] W. Bernreuther, C. Bogner, and O. Dekkers, *The real radiation antenna function for  $S \rightarrow Q\bar{Q}q\bar{q}$  at NNLO QCD*, JHEP **1106** (2011) 032 [[arXiv:1105.0530](#)].
- [21] G. Abelof and A. Gehrmann-De Ridder, *Antenna subtraction for the production of heavy particles at hadron colliders*, JHEP **1104** (2011) 063 [[arXiv:1102.2443](#)].
- [22] A. Gehrmann-De Ridder, E. W. N. Glover, and J. Pires, *Real-Virtual corrections for gluon scattering at NNLO*, JHEP **1202** (2012) 141 [[arXiv:1112.3613](#)].
- [23] G. Abelof and A. Gehrmann-De Ridder, *Double real radiation corrections to  $t\bar{t}$  production at the LHC: the all-fermion processes*, JHEP **1204** (2012) 076 [[arXiv:1112.4736](#)].
- [24] G. Abelof and A. Gehrmann-De Ridder, *Double real radiation corrections to  $t\bar{t}$  production at the LHC: the  $gg \rightarrow t\bar{t}q\bar{q}$  channel* JHEP **1211** (2012) 074 [[arXiv:1207.6546](#)].
- [25] G. Abelof, O. Dekkers, and A. Gehrmann-De Ridder, *Antenna subtraction with massive fermions at NNLO: Double real initial-final configurations*, JHEP **1212** (2012) 107 [[arXiv:1210.5059](#)].
- [26] S. Weinzierl, *Subtraction terms at NNLO*, JHEP **0303** (2003) 062 [[hep-ph/0302180](#)].
- [27] S. Frixione and M. Grazzini, *Subtraction at NNLO*, JHEP **0506** (2005) 010 [[hep-ph/0411399](#)].

- [28] G. Somogyi, Z. Trocsanyi, and V. Del Duca, *A subtraction scheme for computing QCD jet cross sections at NNLO: Regularization of doubly-real emissions*, JHEP **0701** (2007) 070 [[hep-ph/0609042](#)].
- [29] G. Somogyi and Z. Trocsanyi, *A Subtraction scheme for computing QCD jet cross sections at NNLO: Integrating the subtraction terms. I.*, JHEP **0808** (2008) 042 [[arXiv:0807.0509](#)].
- [30] S. Catani and M. Grazzini, *An NNLO subtraction formalism in hadron collisions and its application to Higgs boson production at the LHC*, Phys. Rev. Lett. **98** (2007) 222002 [[hep-ph/0703012](#)].
- [31] C. Anastasiou, K. Melnikov, and F. Petriello, *A New method for real radiation at NNLO*, Phys. Rev. D **69** (2004) 076010 [[hep-ph/0311311](#)].
- [32] T. Binoth and G. Heinrich, *Numerical evaluation of phase space integrals by sector decomposition*, Nucl. Phys. B **693** (2004) 134 [[hep-ph/0402265](#)].
- [33] C. Anastasiou, F. Herzog, and A. Lazopoulos, *On the factorization of overlapping singularities at NNLO*, JHEP **1103** (2011) 038 [[arXiv:1011.4867](#)].
- [34] I. Bierenbaum, M. Czakon, and A. Mitov, *The singular behavior of one-loop massive QCD amplitudes with one external soft gluon*, Nucl. Phys. B **856** (2012) 228 [[arXiv:1107.4384](#)].
- [35] M. Czakon, A. Mitov, and S. Moch, *Heavy-quark production in massless quark scattering at two loops in QCD*, Phys. Lett. B **651** (2007) 147 [[arXiv:0705.1975](#)].
- [36] M. Czakon, A. Mitov, and S. Moch, *Heavy-quark production in gluon fusion at two loops in QCD*, Nucl. Phys. B **798** (2008) 210 [[arXiv:0707.4139](#)].
- [37] R. Bonciani, A. Ferroglia, T. Gehrmann, D. Maitre, and C. Studerus, *Two-Loop Fermionic Corrections to Heavy-Quark Pair Production: The Quark-Antiquark Channel*, JHEP **0807** (2008) 129 [[arXiv:0806.2301](#)].
- [38] R. Bonciani, A. Ferroglia, T. Gehrmann, and C. Studerus, *Two-Loop Planar Corrections to Heavy-Quark Pair Production in the Quark-Antiquark Channel*, JHEP **0908** (2009) 067 [[arXiv:0906.3671](#)].
- [39] R. Bonciani, A. Ferroglia, T. Gehrmann, A. von Manteuffel, and C. Studerus, *Two-Loop Leading Color Corrections to Heavy-Quark Pair Production in the Gluon Fusion Channel*, JHEP **1101** (2011) 102 [[arXiv:1011.6661](#)].
- [40] S. Laporta and E. Remiddi, *The analytical value of the electron ( $g - 2$ ) at order  $\alpha^3$  in QED*, Phys. Lett. B **379** (1996) 283 [[hep-ph/9602417](#)];
- [41] S. Laporta, *High-precision calculation of multi-loop Feynman integrals by difference equations*, Int. J. Mod. Phys. A **15** (2000) 5087 [[hep-ph/0102033](#)];
- [42] F.V. Tkachov, *A Theorem On Analytical Calculability Of Four Loop Renormalization Group Functions*, Phys. Lett. B **100** (1981) 65.
- [43] K.G. Chetyrkin and F.V. Tkachov, *Integration By Parts: The Algorithm To Calculate Beta Functions In 4 Loops*, Nucl. Phys. B **192** (1981) 159.
- [44] A. V. Kotikov, *Differential equations method: New technique for massive Feynman diagrams calculation*, Phys. Lett. B **254** (1991) 158.
- [45] A. V. Kotikov, *Differential equations method: The Calculation of vertex type Feynman diagrams*, Phys. Lett. B **259** (1991) 314.

- [46] A. V. Kotikov, *Differential equation method: The Calculation of  $N$  point Feynman diagrams*, Phys. Lett. B **267** (1991) 123.
- [47] E. Remiddi, *Differential equations for Feynman graph amplitudes*, Nuovo Cim. A **110** (1997) 1435 [[hep-th/9711188](#)].
- [48] M. Caffo, H. Czyz, S. Laporta, and E. Remiddi, *Master equations for master amplitudes*, Acta Phys. Polon. B **29** (1998) 2627 [[hep-th/9807119](#)].
- [49] M. Caffo, H. Czyz, S. Laporta, and E. Remiddi, *The master differential equations for the 2-loop sunrise selfmass amplitudes*, Nuovo Cim. A **111** (1998) 365 [[hep-th/9805118](#)].
- [50] T. Gehrmann and E. Remiddi, *Differential equations for two-loop four-point functions*, Nucl. Phys. B **580** (2000) 485 [[hep-ph/9912329](#)].
- [51] M. Argeri and P. Mastrolia, *Feynman Diagrams and Differential Equations*, Int. J. Mod. Phys. A **22** (2007) 4375 [[arXiv:0707.4037](#)].
- [52] C. Bauer, A. Frink, and R. Kreckel, *Introduction to the GiNaC Framework for Symbolic Computation within the C++ Programming Language*, J. Symbolic Computation **33** (2002) 1 [[cs.sc/0004015](#)].
- [53] R. H. Lewis, *Computer Algebra System Fermat*, <http://www.bway.net/lewis>.
- [54] C. Studerus, *Reduze - Feynman Integral Reduction in C++*, Comput. Phys. Commun. **181** (2010) 1293 [[arXiv:0912.2546](#)].
- [55] A. von Manteuffel and C. Studerus, *Reduze 2 - Distributed Feynman Integral Reduction*, [arXiv:1201.4330](#).
- [56] A. B. Goncharov, *Multiple polylogarithms, cyclotomy, and modular complexes*, Math. Res. Lett. **5** (1998) 497, [[arXiv:1105.2076](#)].
- [57] A. B. Goncharov, *Galois symmetries of fundamental groupoids and noncommutative geometry*, Duke Math J. **128 no. 2** (2005) 209, [[math/0208144](#)].
- [58] T. Gehrmann and E. Remiddi, *Two loop master integrals for  $\gamma^* \rightarrow 3$  jets: The planar topologies*, Nucl. Phys. B **601** (2001) 248 [[hep-ph/0008287](#)].
- [59] T. Gehrmann and E. Remiddi, *Numerical evaluation of two-dimensional harmonic polylogarithms*, Comput. Phys. Commun. **144** (2002) 200 [[hep-ph/0111255](#)].
- [60] A. B. Goncharov, *Multiple polylogarithms, cyclotomy and modular complexes* Math. Res. Lett. **5** (1998), 497-516.
- [61] D. J. Broadhurst, *Massive 3-loop Feynman diagrams reducible to  $SC^*$  primitives of algebras of the sixth root of unity*, Eur. Phys. J. C **8** (1999) 311 [[hep-th/9803091](#)].
- [62] E. Remiddi and J.A.M. Vermaseren, *Harmonic polylogarithms*, Int. J. Mod. Phys. A **15** (2000) 725 [[hep-ph/9905237](#)].
- [63] T. Gehrmann and E. Remiddi, *Numerical evaluation of harmonic polylogarithms*, Comput. Phys. Commun. **141** (2001) 296 [[hep-ph/0107173](#)].
- [64] J. Vollinga and S. Weinzierl, *Numerical evaluation of multiple polylogarithms*, Comput. Phys. Commun. **167** (2005) 177 [[hep-ph/0410259](#)].
- [65] D. Maître, *HPL, a mathematica implementation of the harmonic polylogarithms*, Comput. Phys. Commun. **174** (2006) 222 [[hep-ph/0507152](#)].

- [66] D. Maître, *Extension of HPL to complex arguments*, Comput. Phys. Commun. **183** (2012) 846 [[hep-ph/0703052](#)].
- [67] S. Buehler and C. Duhr, *CHAPLIN - Complex Harmonic Polylogarithms in Fortran*, [arXiv:1106.5739](#).
- [68] A. von Manteuffel and C. Studerus, *Top quark pairs at two loops and Reduze 2*, PoS LL **2012** (2012) 059 [[arXiv:1210.1436](#)].
- [69] A. von Manteuffel and C. Studerus, *Massive planar and non-planar double box integrals for light  $N_f$  contributions to  $gg \rightarrow t\bar{t}$* , [arXiv:1306.3504](#).
- [70] S. Borowka and G. Heinrich, *Massive non-planar two-loop four-point integrals with SecDec 2.1*, Comput. Phys. Commun. **184** (2013) 2552 [[arXiv:1303.1157](#)].
- [71] A. B. Goncharov, M. Spradlin, C. Vergu, and A. Volovich, *Classical Polylogarithms for Amplitudes and Wilson Loops*, Phys. Rev. Lett. **105** (2010) 151605 [[arXiv:1006.5703](#)].
- [72] F. Brown, *On the decomposition of motivic multiple zeta values*, [arXiv:1102.1310](#).
- [73] L. J. Dixon, J. M. Drummond, and J. M. Henn, *Bootstrapping the three-loop hexagon*, JHEP **1111** (2011) 023 [[arXiv:1108.4461](#)].
- [74] C. Duhr, H. Gangl, and J. R. Rhodes, *From polygons and symbols to polylogarithmic functions*, JHEP **1210** (2012) 075 [[arXiv:1110.0458](#)].
- [75] L. J. Dixon, J. M. Drummond, and J. M. Henn, *Analytic result for the two-loop six-point NMHV amplitude in  $N=4$  super Yang-Mills theory*, JHEP **1201** (2012) 024 [[arXiv:1111.1704](#)].
- [76] C. Duhr, *Hopf algebras, coproducts and symbols: an application to Higgs boson amplitudes*, JHEP **1208** (2012) 043, [[arXiv:1203.0454](#)].
- [77] L. J. Dixon, C. Duhr, and J. Pennington, *Single-valued harmonic polylogarithms and the multi-Regge limit*, JHEP **1210** (2012) 074, [[arXiv:1207.0186](#)].
- [78] J. Drummond, *Generalised ladders and single-valued polylogarithms*, JHEP **1302** (2013) 092, [[arXiv:1207.3824](#)].
- [79] F. Chavez and C. Duhr, *Three-mass triangle integrals and single-valued polylogarithms*, JHEP **1211** (2012) 114, [[arXiv:1209.2722](#)].
- [80] T. Gehrmann, L. Tancredi, and E. Weihs, *Two-loop QCD helicity amplitudes for  $gg \rightarrow Zg$  and  $gg \rightarrow Z\gamma$* , JHEP **1304** (2013) 101 [[arXiv:1302.2630](#)].
- [81] C. Anastasiou, C. Duhr, F. Dulat, and B. Mistlberger, *Soft triple-real radiation for Higgs production at N<sup>3</sup>LO*, JHEP **1307** (2013) 003 [[arXiv:1302.4379](#)].
- [82] J. Golden, A. B. Goncharov, M. Spradlin, C. Vergu, and A. Volovich, *Motivic Amplitudes and Cluster Coordinates*, [arXiv:1305.1617](#).
- [83] T. Gehrmann, L. Tancredi, and E. Weihs, *Two-loop master integrals for  $q\bar{q} \rightarrow VV$ : the planar topologies*, JHEP **1308** (2013) 070 [[arXiv:1306.6344](#)].
- [84] J. M. Henn and V. A. Smirnov, *Analytic results for two-loop master integrals for Bhabha scattering I*, [arXiv:1307.4083](#).
- [85] L. J. Dixon, J. M. Drummond, M. von Hippel, and J. Pennington, *Hexagon functions and the three-loop remainder function*, [arXiv:1308.2276](#).

- [86] P. Nason, S. Dawson, and R. K. Ellis, *The Total Cross-Section for the Production of Heavy Quarks in Hadronic Collisions*, Nucl. Phys. B **303**, (1988) 607.
- [87] W. Beenakker, H. Kuijf, W. L. van Neerven, and J. Smith, *QCD Corrections to Heavy Quark Production in  $p$  anti- $p$  Collisions*, Phys. Rev. D **40** (1989) 54.
- [88] J. G. Körner, Z. Merebashvili, and M. Rogal, *NNLO  $O(\alpha_s^4)$  results for heavy quark pair production in quark-antiquark collisions: The One-loop squared contributions*, Phys. Rev. D **77** (2008) 094011 [Erratum-ibid. D **85** (2012) 119904] [[arXiv:0802.0106](#)].
- [89] B. Kniehl, Z. Merebashvili, J. G. Körner, and M. Rogal, *Heavy quark pair production in gluon fusion at next-to-next-to-leading  $O(\alpha_s^4)$  order: One-loop squared contributions*, Phys. Rev. D **78** (2008) 094013 [[arXiv:0809.3980](#)].
- [90] C. Anastasiou and S. M. Aybat, *The One-loop gluon amplitude for heavy-quark production at NNLO*, Phys. Rev. D **78** (2008) 114006 [[arXiv:0809.1355](#)].
- [91] P. Nogueira, *Automatic Feynman graph generation*, J. Comput. Phys. **105** (1993) 279.
- [92] W. L. van Neerven, *Dimensional Regularization Of Mass And Infrared Singularities In Two Loop On-shell Vertex Functions*, Nucl. Phys. B **268** (1986) 453.
- [93] M. Argeri, P. Mastrolia, and E. Remiddi, *The analytic value of the sunrise self-mass with two equal masses and the external invariant equal to the third squared mass*, Nucl. Phys. B **631** (2002) 388 [[hep-ph/0202123](#)].
- [94] R. Bonciani, P. Mastrolia, and E. Remiddi, *Vertex diagrams for the QED form factors at the 2-loop level*, Nucl. Phys. B **661** (2003) 289 [Erratum-ibid. B **702** (2004) 359] [[hep-ph/0301170](#)].
- [95] R. Bonciani, P. Mastrolia, and E. Remiddi, *Master Integrals for the 2-loop QCD virtual corrections to the Forward-Backward Asymmetry*, Nucl. Phys. B **690** (2004) 138 [[hep-ph/0311145](#)].
- [96] J. Fleischer, A.V. Kotikov, and O.L. Veretin, *Analytic two-loop results for selfenergy- and vertex-type diagrams with one non-zero mass*, Nucl. Phys. B **547** (1999) 343 [[hep-ph/9808242](#)].
- [97] U. Aglietti and R. Bonciani, *Master integrals with one massive propagator for the two-loop electroweak form factor*, Nucl. Phys. B **668** (2003) 3 [[hep-ph/0304028](#)].
- [98] A.I. Davydychev and M.Y. Kalmykov, *Massive Feynman diagrams and inverse binomial sums*, Nucl. Phys. B **699** (2004) 3 [[hep-th/0303162](#)].
- [99] U. Aglietti and R. Bonciani, *Master integrals with 2 and 3 massive propagators for the 2-loop electroweak form factor: Planar case*, Nucl. Phys. B **698** (2004) 277 [[hep-ph/0401193](#)].
- [100] M. Czakon, J. Gluza, and T. Riemann, *Master integrals for massive two-loop Bhabha scattering in QED*, Phys. Rev. D **71** (2005) 073009 [[hep-ph/0412164](#)].
- [101] G. Bell, *Higher order QCD corrections in exclusive charmless B decays*, doctoral thesis, LMU Munich, 2006, [arXiv:0705.3133](#).
- [102] R. Bonciani and A. Ferroglia, *Two-Loop QCD Corrections to the Heavy-to-Light Quark Decay*, JHEP **0811** (2008) 065 [[arXiv:0809.4687](#)].
- [103] A. von Manteuffel, R. M. Schabinger, and H. X. Zhu, *The Complete Two-Loop Integrated Jet Thrust Distribution In Soft-Collinear Effective Theory*, [arXiv:1309.3560](#).



- [104] J. Ablinger, J. Blümlein, and C. Schneider, *Harmonic Sums and Polylogarithms Generated by Cyclotomic Polynomials*, *J.Math.Phys.* **52** (2011) 102301, [[arXiv:1105.6063](#)].
- [105] C. Bogner and F. Brown, *Symbolic integration and multiple polylogarithms*, *PoS LL* **2012** (2012) 053 [[arXiv:1209.6524](#)].
- [106] A. von Manteuffel, *A Mathematica package for multiple polylogarithms*, unpublished.
- [107] A. Ferroglia, M. Neubert, B. D. Pecjak, and L. L. Yang, *Two-loop divergences of massive scattering amplitudes in non-abelian gauge theories*, *JHEP* **0911**, 062 (2009) [[arXiv:0908.3676](#)].
- [108] P. Bärnreuther, *Top Quark Pair Production at the LHC*, doctoral thesis, RWTH Aachen, 2012.
- [109] S. Laporta and E. Remiddi, *Analytic treatment of the two loop equal mass sunrise graph*, *Nucl. Phys. B* **704** (2005) 349 [[hep-ph/0406160](#)].
- [110] S. Müller-Stach, S. Weinzierl, and R. Zayadeh, *A Second-Order Differential Equation for the Two-Loop Sunrise Graph with Arbitrary Masses*, *Commun. Num. Theor. Phys.* **6** (2012) 1, 203 [[arXiv:1112.4360](#)].
- [111] L. Adams, C. Bogner, and S. Weinzierl, *The two-loop sunrise graph with arbitrary masses*, [arXiv:1302.7004](#).
- [112] J. Kuipers, T. Ueda, J. A. M. Vermaseren, and J. Vollinga, *FORM version 4.0*, *Comput. Phys. Commun.* **184**, 1453 (2013) [[arXiv:1203.6543](#)].
- [113] J. A. M. Vermaseren, *Axodraw*, *Comput. Phys. Commun.* 83 (1994) 45.